Relaxation properties of persistent current in YBCO-coated conductors

K. Himeki [a], M. Kiuchi [a], E.S. Otabe [a], T. Matsushita* [a,1], S. Miyata [b], A. Ibi [b], Y. Yamada [b], Y. Shiohara [c],

[a] *Faculty of Computer Science and Systems Engineering, Kyushu Institute of Technology, 680–4 Kawazu, Iizuka 820–8502, Japan*

[b] *Superconductivity Research Laboratory, 2–4–1 Mutsuno, Atsuta-ku, Nagoya, 456-8587, Japan*

[c] *Superconductivity Research Laboratory, 1–10–13 Shinonome, Koto-ku, Tokyo, 135-0062, Japan*

Abstract

The relaxation properties were investigated for PLD processed YBCO coated conductors deposited on IBAD substrates in the region of 0.25 – 1.50 μm for the thickness of superconducting layer to clarify the thickness dependence of the relaxation of magnetization. The apparent pinning potential U_0^* was estimated from the relaxation rate. It was found that U_0^* increases with increasing temperature in the low temperature region. The weak thickness dependence of U_0^* in this temperature region comes from the three-dimensional flux pinning mechanism. Then, U_0^* has a peak followed by a decrease with increasing temperature. The peak value of U_0^* increases with increasing thickness. Hence, the thicker superconductor is more advantageous for applications in the middle temperature range and higher. The flux pinning mechanism in the medium and higher temperature region is two-dimensional and the larger U_0^* value in the thicker specimen originates mainly from the thickness. For the improvement of U_0^* in the low temperature region, it is required to enhance the flux pinning strength and to increase the thickness without deterioration in the critical current density.

Keywords: YBCO, thickness, relaxation, U_0^*, flux creep-flow model
PACS: 74.25.Qt, 74.25.Sv, 74.72.Bk

[1] Corresponding author.
T. Matsushita
Postal address: Department of Computer Science and Electronics, Kyushu Institute of Technology, 680–4, Kawazu, Iizuka 820–8502 Japan

1 Introduction

Various applications of $YBa_2Cu_3O_{7-\delta}$ (YBCO) tapes at low and medium temperatures and at high magnetic fields are expected because of very high critical current density. Candidates for such applications are superconducting magnets for nuclear magnetic resonance (NMR) and superconducting magnetic energy storage (SMES), etc. For these applications, the stability of superconducting persistent current is a fundamental issue.

It is known that the superconducting current originated from the flux pinning mechanism is not a true persistent current but decreases with time due to thermal activation of pinned flux lines. This phenomenon is caused by the flux creep. For this reason, it is necessary to improve the relaxation properties of the pinning current in YBCO tapes for application to equipments operating in a persistent current mode.

The important parameter in the flux creep is the pinning potential, U_0. It is known that U_0 has a dependence on the thickness of superconducting layer in the two-dimensional pinning regime. Hence, it seems to be important to investigate the relaxation property of superconducting current for coated tapes with different superconducting layer thickness. In fact, it was reported that the n-value is larger for thicker superconducting layer in the low electric field region at low temperatures [1]. In this paper, the thickness dependence of relaxation of IBAD/PLD processed YBCO tapes is investigated in the range of $0.25 - 1.5$ μm.

Phone: +81–948–29–7663; Fax: +81–948–29–7661
E-mail address: matusita@cse.kyutech.ac.jp

2 Experiments

The specimens were PLD-processed YBCO-coated conductor deposited on IBAD substrate with GZO inner layer and CeO_2 cap layer [2]. The thicknesses of YBCO layer were 0.25, 0.50, 1.00 and 1.50 μm. The specifications of these specimens are listed in Table 1.

The DC magnetization and its relaxation were measured by a SQUID magnetometer in a magnetic field parallel to the c-axis of the specimen. Measurements were done up to 7 T over the temperature region of $5-70$ K. E-J characteristics were estimated from the relaxation measurements and J_{c}-B characteristics were estimated with the electric field criterion of $E_{\mathrm{c}} = 10^{-9}$ V/m. From the logarithmic relaxation rate of the magnetization, the apparent pinning potential U_0^* was estimated:

$$-\frac{\mathrm{d}}{\mathrm{dlog}t}\left(\frac{M}{M_0}\right) = \frac{U_0^*}{k_{\mathrm{B}}T}. \tag{1}$$

The initial magnetization M_0 was determined by extrapolating the relaxation curve from the time range of $10^2 - 10^3$ s to $t = 1$ s.

3 Theory

The critical current properties were analyzed using the flux creep-flow model [3]. In the virtual flux-creep free case, the critical current density takes a value determined only by the flux pinning and its temperature and magnetic field dependence is assumed as

$$J_{\mathrm{c0}} = A\left(1-\frac{T}{T_{\mathrm{c}}}\right)^m B^{\gamma-1}\left(1-\frac{B}{B_{\mathrm{c2}}}\right)^2, \tag{2}$$

where A, m, γ are pinning parameters. The pinning potential U_0 depends on J_{c0}. The superconducting layers thickness d is also a key factor which determines U_0, and U_0 is proportional to d in the two-dimensional pinning regime, while U_0 is independent of d in the three-dimensional pinning regime:

$$\begin{aligned} U_0 &= \frac{0.835 g^2 k_{\mathrm{B}} J_{\mathrm{c0}}^{1/2}}{(2\pi)^{3/2} B^{1/4}}; \quad d > L, \\ &= \frac{4.23 g^2 k_{\mathrm{B}} J_{\mathrm{c0}} d}{2\pi B^{1/2}}; \quad d < L. \end{aligned} \tag{3}$$

In the above L is the pinning correlation length is given by

$$L = \left(\frac{B a_{\mathrm{f}}}{2\pi \mu_0 J_{\mathrm{c0}}} \right)^{1/2} \tag{4}$$

with a_{f} denoting the flux line spacing. It should be noted that even if the pinning is in the three-dimensional case at low magnetic fields for fairly thick superconductor, the pinning may change to the two-dimensional one at high magnetic fields due to the increase in L with decreasing J_{c0}. The parameter g^2 is the number of flux lines in a flux bundle, and is proposed to be given by

$$g^2 = g_{\mathrm{e}}^2 \left[\frac{5 k_{\mathrm{B}} T}{2 U_{\mathrm{e}}} \log \left(\frac{B a_{\mathrm{f}} \nu_0}{E_{\mathrm{c}}} \right) \right]^{4/3} \tag{5}$$

so that the critical current density under the flux creep is maximized [4]. In the above g_e^2 is the maximum value of g^2 for the perfect three-dimensional triangular flux line lattice, U_e is the pinning potential when $g = g_e$, E_c is the electric field criterion to determine J_c, and ν_0 is the attempt frequency of the flux bundle. g_e^2 is given by

$$g_{\mathrm{e}}^2 = \frac{C_{66}}{2\pi J_{\mathrm{c0}} B a_{\mathrm{f}}}, \tag{6}$$

where C_{66} is the shear modulus of flux line lattice. In practical superconductors the flux pinning strength is statistically distributed. Here it is simply assumed that only the parameter A which represents the pinning strength is distributed as

$$f(A) = K \exp\left[-\frac{(\log A - \log A_{\rm m})^2}{2\sigma^2}\right], \tag{7}$$

where $A_{\rm m}$ is the most probable value of A and σ^2 is a parameter representing a distribution width and K is a normalization constant. The electric field E caused by flux creep and flow is calculated as a function of the current density J and averaged with respect to the distributed A. The details of the theoretical calculation are described elsewhere [3]. The theoretical critical current density is determined from the obtained E-J curve with the same electric field criterion of $E_{\rm c} = 10^{-9}$ V/m as done in experiments. The pinning parameters $A_{\rm m}$, σ, m γ and g^2 are determined so that the calculated E-J curves agree with the experiments.

E-J characteristics is also evaluated experimentally by magnetic relaxation. In the external magnetic field normal to the tape surface, the current density J is estimated by the magnetic moment $m_{\rm m}$ using the Bean-London model:

$$J = \frac{12 m_{\rm m}}{w^2 d(3l - w)}, \tag{8}$$

where l, w and d are length, width and thickness of the specimen, respectively.

The electric field E can be estimated from the relaxation of the magnetic moment as

$$E = -\frac{\mu_0 G}{2d(l + w)} \cdot \frac{{\rm d}m_{\rm m}}{{\rm d}t}, \tag{9}$$

where G is a factor determined by the geometry [5].

4 Results and Discussion

Fig. 1 shows the J_c-B characteristics of the four specimens at 20, 50 and 70 K in the magnetic field ranges of (a) $0 - 6.5$ T and (b) $0 - 1.25$ T, respectively. It is found that J_c decreases with increasing thickness at low magnetic fields except for specimen #4. This comes directly from the structural degradation of the superconducting layer such as porosities and/or a-axis aligned grains in thick specimen. However, it is found that J_c of the thinnest specimen decreased rapidly with increasing magnetic field due to the strong influence of the flux creep. Fig. 2 (a) shows the relaxation of normalized magnetization for specimen #1 at 1 T in the temperature region of $5 - 60$ K. The relaxation rate increases monotonically with increasing temperature. Fig. 2 (b) shows the relaxation of magnetization of the four specimens at 1 T at 60 K. It is found that the relaxation late increases generally with decreasing thickness. This phenomenon is directly associated with the dependence of the pinning potential on the thickness of superconducting layer. The E-J curves of specimen #1 obtained from the relaxation of magnetization are shown in Fig. 3.

The apparent pinning potential, U_0^*, is the value of activation energy extrapolated linearly from the measurement point to $J = 0$, and is usually smaller than the real pinning potential, U_0. Especially, it is known that U_0^* reduces to zero at $T = 0$. For example, Welch [6] argued the effect of the shape of pinning potential on U_0^* and derived theoretically:

$$U_0^* = 1.65(k_{\mathrm{B}} T U_0^2)^{1/3}. \tag{10}$$

The temperature dependence of U_0^* at 1 T obtained from the relaxation rate of the four specimens is shown in Fig. 4. In the low temperature region U_0^* increases linearly with temperature and only weakly depends on the thickness.

Then, U_0^* has a peak followed by a decrease with further increase in temperature. It is found that the peak temperature is almost unchanged for specimens #1 - #3, while that of specimen #4 is higher than others. The result on a melt-processed bulk YBCO [6] is also shown in Fig. 4 for comparison.

The behavior that U_0^* approaches zero at $T = 0$ was partly ascribed to the shape of the pinning potential well as described by Eq. (10). However, the prediction of Eq. (10) leads to the larger U_0^* value at low temperatures than observed. This seems to be attributed to the neglect of the distribution of the flux pinning strength A and the reduction in g^2 from g_{e}^2 [7].

The pinning parameters obtained from the E-J curves are listed in Table 2. The value of A_{m} increases with decreasing thickness except for #4 due to the structural degradation of the superconducting layer. It is found that σ^2 increases with decreasing thickness. The theoretical results of E-J curves and the J_{c} characteristics are compared with experiments in Figs. 3 and 5, respectively. It can be seen that agreement is satisfactory. The pinning potential U_0^* estimated with the obtained pining parameters are compared with experiments in Fig. 6.

In the low temperature region, the flux pinning is three-dimensional and the pinning potential given by Eq. (3) is proportional to $g^2 A_{\mathrm{m}}^{1/2}$. Hence, U_0^* is proportional to $A_{\mathrm{m}}^{1/3}$ due to $g^2 = 1$ for the whole specimens. For this reason, the value of U_0^* at low temperature is not so much different among specimens.

In the medium temperature region, the value of U_0^* becomes to be dependent on the thickness, deviating from the linear relationship with temperature. This indicates that the flux pinning changes from three-dimensional to two-dimensional due to the increase in pinning correlation length L over the thickness. In the two-dimensional pinning regime, the pinning potential given by Eq. (3) is proportional to $g^2 A_\mathrm{m} d$. The value of A_m decreases gradually and the value of g^2 increases with the thickness d as can be seen from Table 2. Eq. (6) leads to that g^2 is proportional to $g_\mathrm{e}^{-2/3}$ and hence to $J_\mathrm{c0}^{-1/3}$. Thus, the thickness dependence of g^2 given in Table 2 can be explained from the negative correlation between A_m and d. As a result, the increase in U_0^* with increasing d in the medium and high temperature region can be explained. Since the dimensional cross-over of flux pinning occurs at lower temperature in the thinner specimen, the thicker specimen is more advantageous. Specimen #4 has a fairly high critical current density, although it is thick. Hence, the change in the flux pinning mechanism from three-dimensional to two-dimensional occurs at high temperature. This causes the high peak value of U_0^*.

However, the deviation of the theoretical result of U_0^* from experiments becomes larger at higher temperature. This simply comes from the present assumption that σ^2 is kept constant up to high temperatures. It is natural that the distribution width of J_c0 becomes relatively larger, if the distribution originates from the nonuniform critical temperature.

For realization of applications of YBCO coated conductors in a persistent current mode, it is necessary to increase U_0^* to a sufficient value especially at low temperatures. For this purpose, it seems to be important to enhance the flux pinning strength and introduction of strong artificial pinning centers is desirable. In addition, it is necessary to increase superconducting thickness without deterioration in the critical current density.

5 Summary

The magnetic relaxation property was investigated for YBCO tapes made by the IBAD/PLD process of superconducting thickness of 0.25, 0.50, 1.00 and 1.50 μm to clarify the superconducting thickness dependence of relaxation. It is found that the apparent pinning potential U_0^* increases with increasing temperature in the low temperature region followed by a decrease. In this region U_0^* is rather insensitive to the thickness of the superconductor, since it is predicted to be proportional to $A_{\mathrm{m}}^{1/3}$ in the three-dimensional pinning regime. In the medium temperature region, U_0^* has a peak which becomes higher with increasing thickness. In this temperature region the flux pinning is considered to be in two-dimensional regime. This thickness dependence can be explained by the theoretical model of flux creep and flow.

For the improvement of U_0^* especially at low temperatures, it is required to enhance the flux pinning strength. For this purpose introduction of strong artificial pinning centers seems to be effective. In addition, it is necessary to increase the superconducting layer thickness larger than the pinning correlation length without deterioration in the critical current density.

6 Acknowledgement

This work is partly supported by the New Energy and Technology Development Organization (NEDO) as Collaborative Research and Development of Fundamental Technologies for Superconductivity Applications.

References

[1] K. Kimura, M. Kiuchi, E.S. Otabe, T. Matsushita, S. Miyata, A. Ibi, Y. Yamada, Y. Shiohara, Physica C 463–465 (2007) 697.

[2] T. Muroga, H. Iwai, Y. Yamada, T. Izumi, Y. Shiohara, Y. Iijima, T. Saito, T. Kato, Y. Sugawara, T. Hiroyama, Physica C 392–396 (2003) 796.

[3] M. Kiuchi, K. Noguchi, T. Matsushita, T. Hikata, K. Sato, Physica C 278 (1997) 62.

[4] T. Matsushita, Physica C 217 (1993) 461.

[5] Y. Fukumoto, M. Kiuchi, E.S. Otabe, T. Matsushita, H. Sawa, M. Inoue, T. Kiss, Y. Iijima, K. Kakimoto, T. Saitoh, Physica C 412 (2004) 1036.

[6] D.O. Welch, IEEE Trans. Magn. 27 (1991) 1133.

[7] T. Matsushita, Flux pinning in superconductors, Springer, Berlin, 2006, P.456.

Table 1: Specifications of specimens.

Specimen	Thickness d (μm)	$T_{\rm c}$ (K)
#1	0.25	88.6
#2	0.50	90.1
#3	1.00	86.7
#4	1.50	87.9

Table 2 : Pinning parameters of specimens in (a)low temperature region and (b)high temperature redion, respectively.

(a)	$A_{\rm m}$	σ^2	γ	m	g^2	temperature region
#1	5.0×10^{11}	0.015	0.63	1.50	1.0	$5 - 30$ K
#2	3.5×10^{11}	0.013	0.60	2.00	1.0	$5 - 30$ K
#3	1.8×10^{11}	0.007	0.60	1.89	1.0	$5 - 30$ K
#4	4.0×10^{11}	0.006	0.74	2.98	1.0	$5 - 30$ K

(b)	$A_{\rm m}$	σ^2	γ	m	g^2	temperature region
#1	6.2×10^{12}	0.023	0.64	1.80	2.5	$40 - 60$ K
#2	3.4×10^{11}	0.014	0.64	1.90	2.3	$40 - 60$ K
#3	2.3×10^{11}	0.007	0.65	2.30	1.8	$40 - 70$ K
#4	2.8×10^{11}	0.005	0.70	2.08	1.0	$40 - 70$ K

Figure captions

Fig. 1 J_c-B characteristics obtained by SQUID magnetometer in the magnetic field ranges of (a) 0 – 6.50 T and (b) 0 – 1.25 T at 20, 50 and 70 K.

Fig. 2 (a)Relaxation of magnetization of specimen #1 at 1 T in the temperature range of 5 – 70 K, and (b)relaxation of magnetization of four specimens at 1 T and at 60 K.

Fig. 3 E-J characteristics of specimen #1 at 1 T in the temperature range of 5 – 70 K. Symbols and lines represent the experimental and theoretical results, respectively.

Fig. 4 Temperature dependence of apparent pinning potential of four specimens and bulk specimen [6] at 1 T in the temperature range of 5 – 70 K.

Fig. 5 J_c-B curves of specimen #1. Symbols and lines represent the experimental and theoretical results, respectively.

Fig. 6 Temperature dependence of apparent pinning potential for (a)specimens #1 and #3 and for (b)specimens #2 and #4 at 1 T in the temperature range of 5 – 70 K. Solid symbols represent the experimental results and open symbols with lines represent the theoretical results.

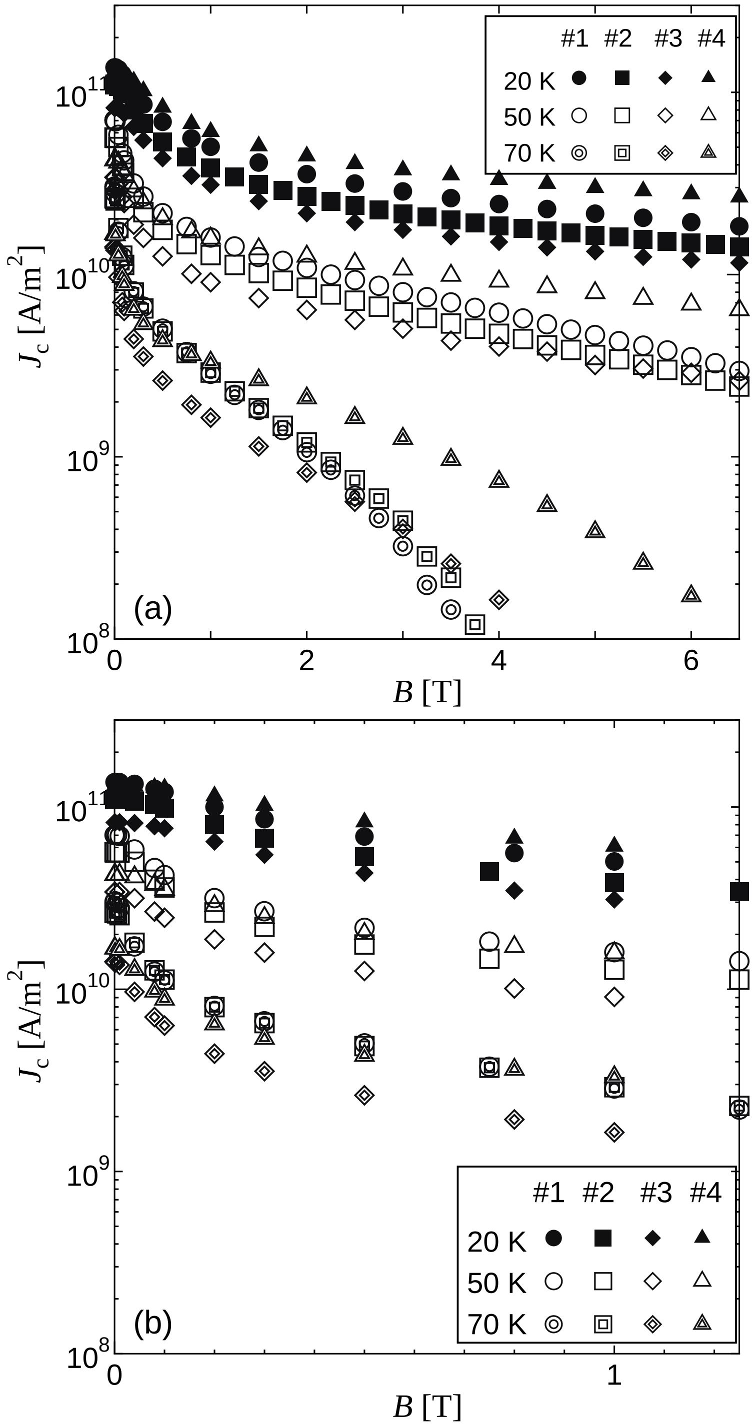

Fig. 1: K. Himeki *et al.* WTP–112/ISS2007

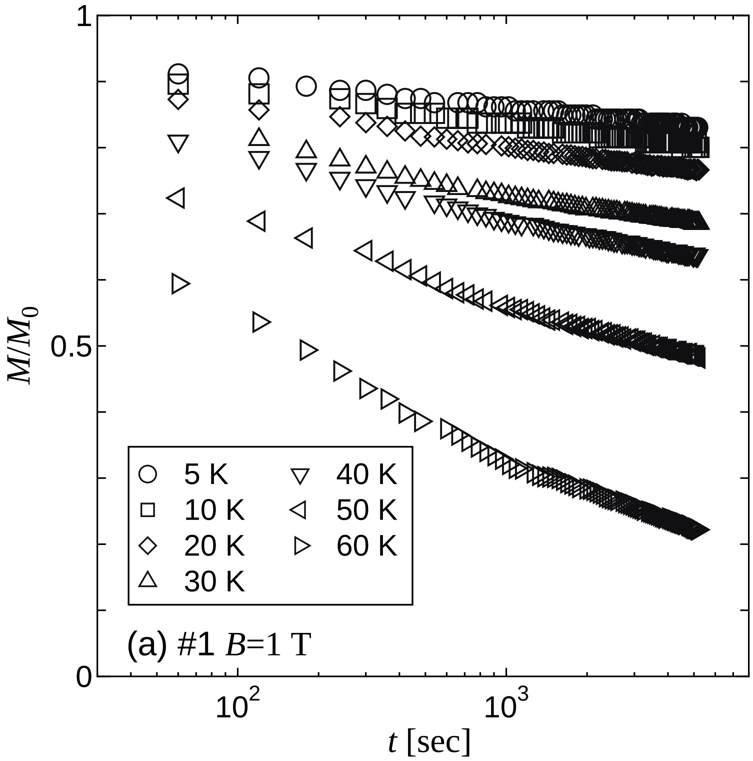

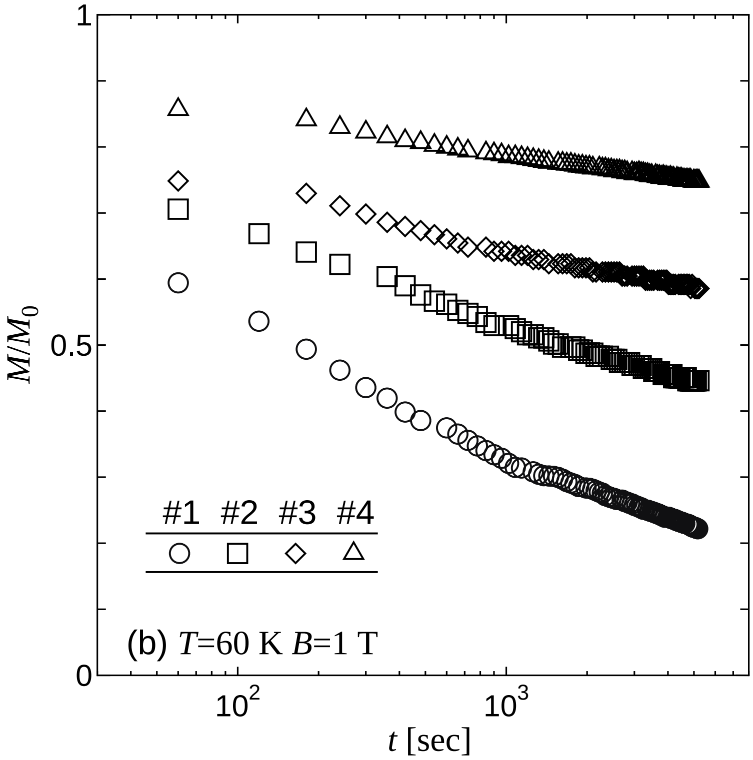

Fig. 2: K. Himeki *et al.* WTP–112/ISS2007

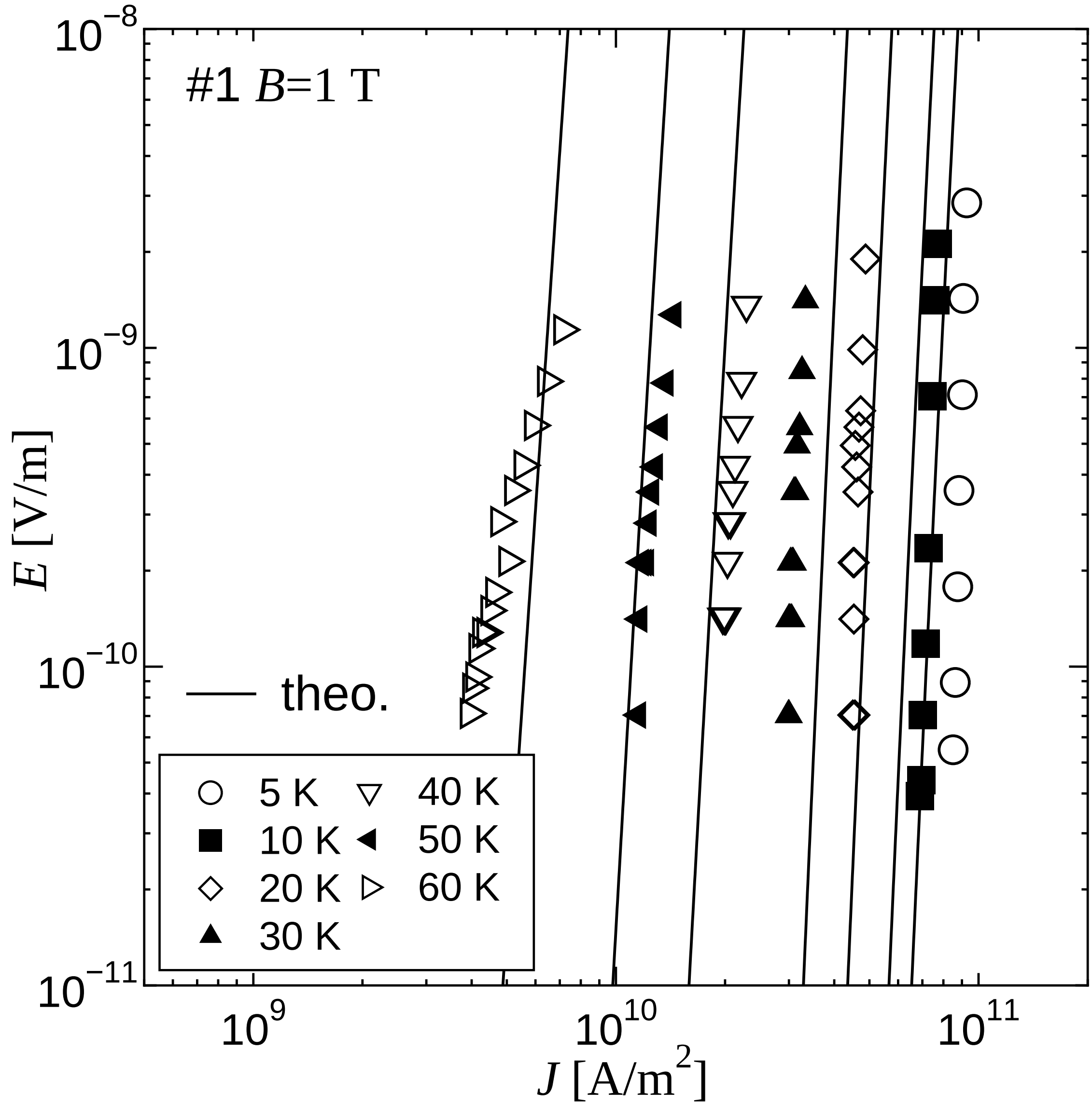

Fig. 3: K. Himeki *et al.* WTP–112/ISS2007

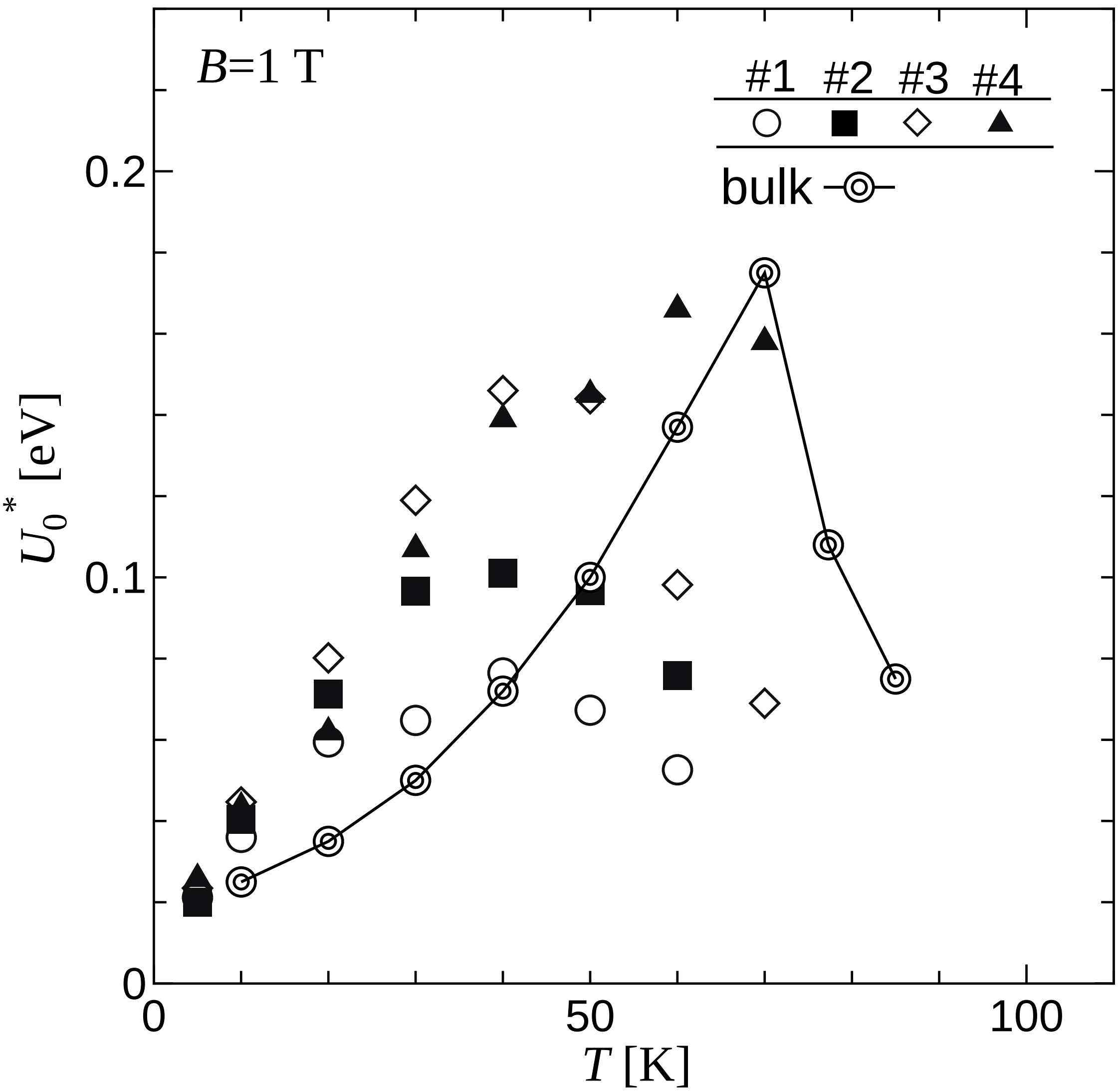

Fig. 4: K. Himeki *et al.* WTP–112/ISS2007

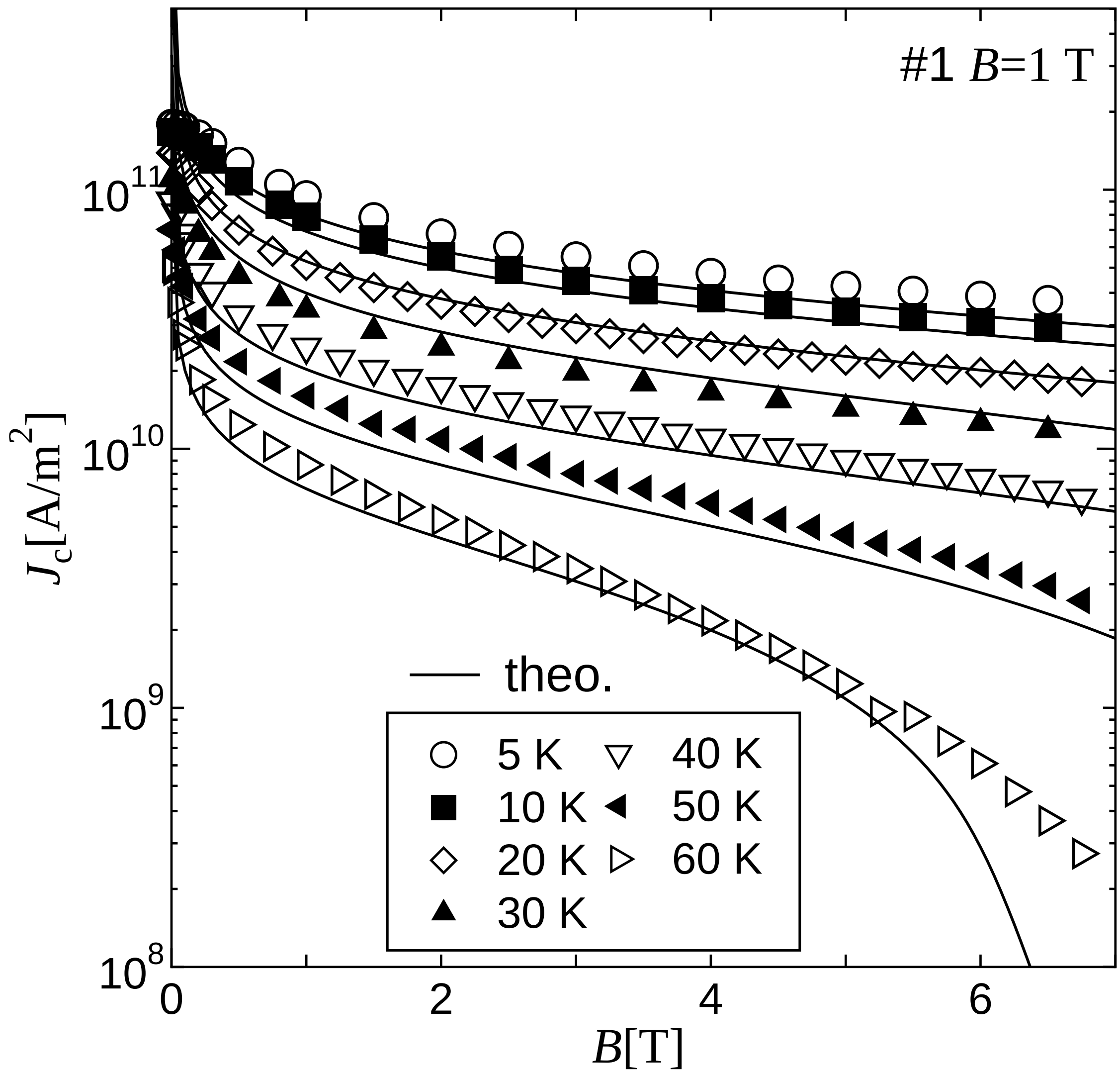

Fig. 5: K. Himeki *et al.* WTP–112/ISS2007

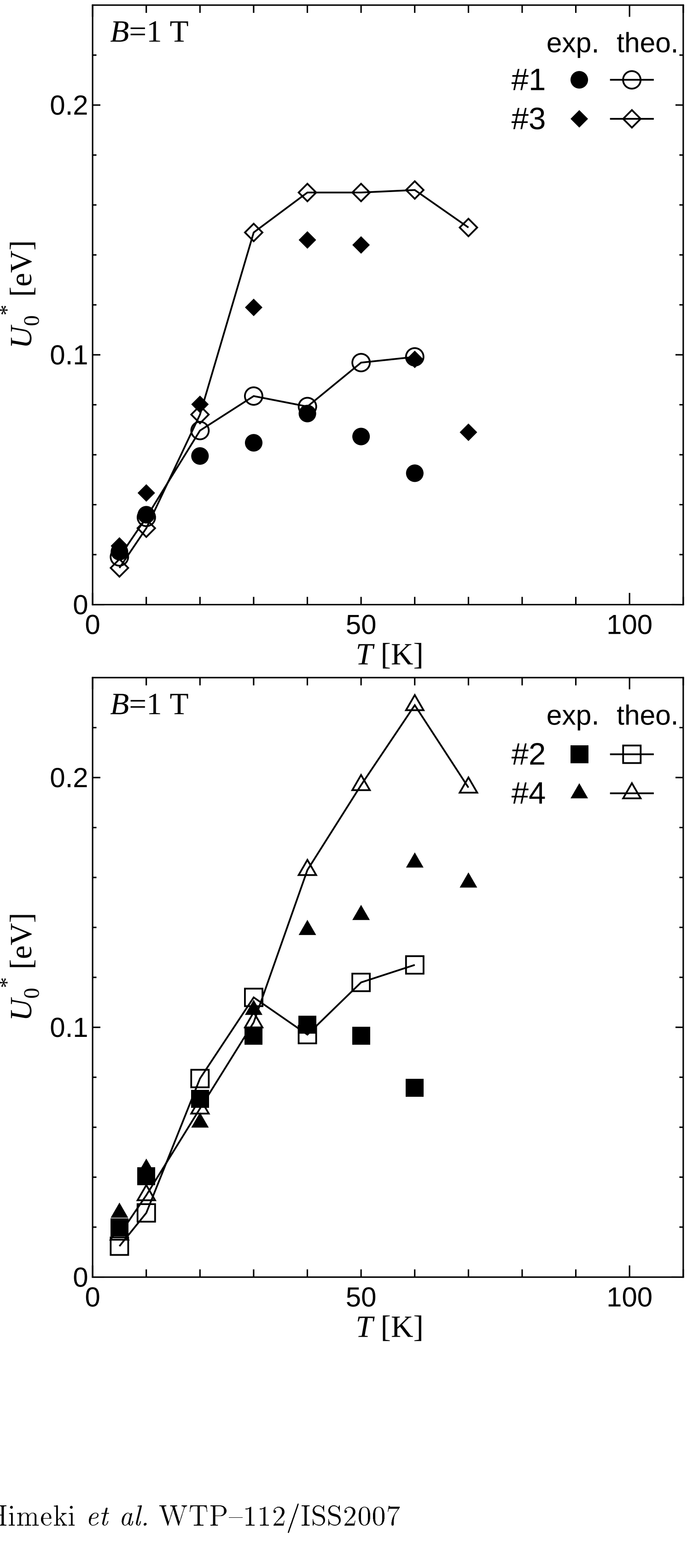

Fig. 6: K. Himeki *et al.* WTP–112/ISS2007